Eur. Phys. J. B **8**, 339–351 (1999)

THE EUROPEAN PHYSICAL JOURNAL B

EDP Sciences

Normal state properties of an interacting large polaron gas

G. De Filippis[1], V. Cataudella[2,a], and G. Iadonisi[2]

[1] Dipartimento di Scienze Fisiche, Università di Salerno, 84081 Baronissi (Salerno), Italy
[2] Dipartimento di Scienze Fisiche, Università di Napoli 80125 Napoli, Italy

Received 13 May 1998

Abstract. A simple approach to the many-polaron problem for both weak and intermediate electron-phonon coupling and valid for densities much smaller than those typical of metals is presented. Within the model the total energy, the collective modes and the single-particle properties are studied and compared with the available theories. It is shown the occurrence of a charge density wave instability in the intermediate coupling regime.

PACS. 71.38.+i Polarons and electron phonon interactions

1 Introduction

The formation of large polarons and bipolarons in polar materials due to Fröhlich interaction with longitudinal optical (LO) phonons has been studied quite extensively since the pioneering work of Landau [1], Pekar [2] and Fröhlich [3] and now it can be considered a well understood problem [4]. However, a large amount of work has been devoted to the simpler single polaron and bipolaron problems neglecting the effect of the polaron-polaron interaction. These effects, on the other hand, are expected to play an important role in heavily doped semiconductors [5] and in many doped perovskites including high T_c superconductors [6,7] that are both characterized by large polar effects and densities much smaller than those typical of metals. In particular, in the case of superconductors infrared absorption measurements suggest the existence of polarons whose properties depend strongly on doping [8].

Recently, the regime characterized by low charge carrier density and strong e-ph interaction has been analyzed. In this regime the formation of a polaron Wigner crystal state is favoured with respect to the metallic phase. The stability of such a state in an ionic dielectric has been studied by the path integral technique pointing out the competition between the dissociation of the polarons at the insulator-metal transition and the melting towards a polaron liquid [9]. Moreover two different approaches are known in literature for the metallic phase of a large polaron system. A perturbative approach, mainly due to Mahan [5,10], makes use of the random phase approximation (RPA) in order to obtain a retarded effective electron-electron (e-e) interaction due to the exchange of LO phonons [11]. A variational approach, due to Devreese [12], is based on an extension of the Lee, Low and Pines (LLP) [13] canonical transformation to the many body problem and is able to give the total energy of the system in terms of the electronic static structure factor. However, both approaches are satisfactory only when electron-phonon (e-ph) effects are weak.

In order to study the many polaron effects in the weak and intermediate e-ph interaction ($\alpha < 7$) and for polaron densities typical of the metallic phase of the doped semiconductors and perovskites we introduce a simple model in which the electron-phonon and the electron-electron interactions are not taken into account at the same level. First the Hamiltonian of two electrons interacting with each other through Coulomb repulsion and with longitudinal optical phonons is introduced and an effective self-consistent electron-electron potential, due to LO phonons exchange, is determined within a variational approach. Then the many body effects are taken into account considering many electrons interacting with each other through the obtained effective potential. Within the proposed model we show that, for weak e-ph interaction, many of the known results can be recovered, while, for intermediate e-ph interaction, we present evidences for a charge density wave instability as suggested by several authors [14,15].

The paper is organized in the following way. In Section 2 the model is introduced and its validity is discussed. The perturbative and the variational approaches are also briefly reviewed. In Section 3 the total energy, the collective excitations and the quasi-particle self-energy are calculated for weak e-ph coupling and are compared with the results obtained within the variational and perturbative approaches. In Section 4 the region of intermediate e-ph interaction is analyzed and numerical results for the single-particle spectral weight function, the collective excitation spectrum and the renormalization coefficient are

[a] e-mail: vit@na.infn.it

presented just above the appearance of the instability signaled by the complete softening of the collective mode.

2 Theoretical framework

In systems characterized by charge carriers coupled with a polar lattice one has to consider the electron-electron interaction and the electron-phonon interaction. The Hamiltonian, which can be used to describe these materials, has the following form [5]:

$$H = H_0 + H_{e-e} + H_{e-ph} \tag{1}$$

where

$$H_0 = \sum_{\mathbf{p}\sigma} E^0(p) c^\dagger_{\mathbf{p}\sigma} c_{\mathbf{p}\sigma} + \sum_{\mathbf{q}} \hbar\omega_l a^\dagger_{\mathbf{q}} a_{\mathbf{q}}$$

$$H_{e-e} = \frac{1}{2V} \sum_{\substack{\mathbf{p_1}\mathbf{p_2}\mathbf{q} \\ \sigma_1\sigma_2}} v_q^\infty c^\dagger_{\mathbf{p}_1+\mathbf{q}\sigma_1} c^\dagger_{\mathbf{p}_2-\mathbf{q}\sigma_2} c_{\mathbf{p}_2\sigma_2} c_{\mathbf{p}_1\sigma_1}$$

$$H_{e-ph} = \sum_{\substack{\mathbf{pq} \\ \sigma}} M_q c^\dagger_{\mathbf{p}+\mathbf{q}\sigma} c_{\mathbf{p}\sigma} \left(a_{\mathbf{q}} + a^\dagger_{-\mathbf{q}}\right)$$

$$v_q^\infty = \frac{v_q}{\epsilon_\infty} = \frac{4\pi e^2}{\epsilon_\infty q^2}.$$

In equation (1) the first term represents the kinetic energy of the electrons with effective band mass m and the energy of the free longitudinal optical phonons; the second term is the Hamiltonian of the electrons interacting with the Coulomb potential screened by the background high frequency dielectric constant ϵ_∞ and the last term describes the electron-phonon interaction whose strength, in the Fröhlich scheme [3], is given by:

$$M_q = -i\hbar\omega_l \frac{R_p^{1/2}}{q} \left(\frac{4\pi\alpha}{V}\right)^{1/2} \tag{2}$$

where α is the Fröhlich coupling constant, $R_p = (\hbar/(2m\omega_l))^{1/2}$ is the polaron radius and V is the volume of the system. In H_{e-e} and in H_{e-ph} the $q = 0$ term is omitted in the sums: *i.e.*, we suppose that the self-energy of an uniform positive charge is subtracted from equation (1). The main properties of the metallic phase of a system described by equation (1) have been discussed within two approaches, proposed by Devreese [12] and Mahan [5,10] respectively. In order to make clearer the comparison with the model which we will discuss, we start with a brief review of the two approaches.

The former is a variational calculation of the ground state energy which makes use of a generalization of the LLP transformation [13] for many polaron systems. The energy per particle of the polaron gas is written as:

$$E_T = E_c + E_p \tag{3}$$

where E_c is the contribution due to the coulomb interaction and E_p represents the e-ph contribution screened by the electrons, which can be expressed in terms of the electronic static structure factor $S(q)$:

$$E_p = -\sum_{\mathbf{q}} \frac{|M_q|^2 S(q)}{\hbar\omega_l + \hbar^2 q^2/(2mS(q))}\,. \tag{4}$$

The latter is a perturbative method of treating the coupled e-ph system and it goes beyond the lowest order processes by using the RPA for the e-e potential which contains the Coulomb repulsion and the e-e interaction mediated by a single phonon exchange:

$$V(q,\omega) = v_q^\infty + M_q^2 D^0(q,\omega) \tag{5}$$

where $D^0(q,\omega)$ is the free LO phonon propagator:

$$D^0(q,\omega) = \frac{1}{\omega - \omega_l + i\eta} - \frac{1}{\omega + \omega_l - i\eta}\,. \tag{6}$$

It is worth noting that the use of the RPA describes the screening of both Coulomb e-e and Fröhlich e-ph interactions, which are treated on the same footing. In the following we will refer to these two models making use of the names variational approach and perturbative approach, respectively.

The model, proposed in this paper, is obtained in the following way.

First we consider the Hamiltonian of two electrons interacting with the longitudinal optical phonons *via* the Fröhlich coupling and repelling each other through the Coulomb force:

$$H = \frac{P^2}{2M} + \frac{p^2}{2\mu} + \frac{e^2}{\epsilon_\infty r} + \sum_{\mathbf{q}} \hbar\omega_l a^\dagger_{\mathbf{q}} a_{\mathbf{q}} + \sum_{\mathbf{k}} \left[M_k \rho_{\mathbf{k}}(\mathbf{r}) e^{i\mathbf{k}\cdot\mathbf{R}} a_{\mathbf{k}} + \text{h.c.}\right] \tag{7}$$

where $\rho_{\mathbf{k}}(\mathbf{r}) = (e^{\frac{i}{2}\mathbf{k}\cdot\mathbf{r}} + \text{h.c.})$, $\mathbf{R}$, $\mathbf{P}$, $\mathbf{r}$, $\mathbf{p}$ are the position and momentum of the centre of mass of the pair and of the relative particle, M and μ are the total and reduced masses respectively. Then we obtain an effective potential for the two electrons of equation (7) eliminating, as we will review briefly, the phonon degrees of freedom. Finally the many body effects are studied considering a system of electrons interacting with this effective potential.

The Hamiltonian (7) commutes with

$$\mathbf{P}_t = \mathbf{P} + \sum_{\mathbf{k}} \hbar\mathbf{k} a^\dagger_{\mathbf{k}} a_{\mathbf{k}} \tag{8}$$

which is the total momentum of the system. The conservation law of the total momentum is taken into account through the unitary transformation:

$$U = \exp\left[i(\mathbf{Q} - \sum_{\mathbf{k}} \mathbf{k} a^\dagger_{\mathbf{k}} a_{\mathbf{k}}) \cdot \mathbf{R}\right] \tag{9}$$

where $\hbar\mathbf{Q}$ is the eigenvalue of $\mathbf{P}_t$. Following LLP [13] we choose the variational trial ground state [16–18] for the transformed Hamiltonian $H_1 = U^{-1}HU$:

$$|\psi\rangle = U_1(\mathbf{r})|0> \varphi(\mathbf{r}) \tag{10}$$

where $|0\rangle$ is the vacuum of $a_{\mathbf{k}}$ and the operator U_1 is given by

$$U_1(\mathbf{r}) = \exp\left[\sum_{\mathbf{k}} (f_{\mathbf{k}}(\mathbf{r})a_{\mathbf{k}} - f^*_{\mathbf{k}}(\mathbf{r})a^\dagger_{\mathbf{k}})\right] . \tag{11}$$

The envelope function $\varphi(\mathbf{r})$ is chosen to be an hydrogenic-like radial wave function:

$$\varphi(\mathbf{r}) = \left[\frac{(2\gamma)^{2\beta+3}}{\Gamma(2\beta+3)}\right]^{1/2} r^\beta e^{-\gamma r} \tag{12}$$

where $\Gamma(x)$ is the Gamma function. The phonon distribution functions $f_{\mathbf{k}}$ are determined in a self-consistent way from a functional variational procedure. In particular, the Eulero-Lagrange equations for the functions $f_{\mathbf{k}}$:

$$\frac{\hbar^2 k^2}{2M} f_{\mathbf{k}} - \frac{\hbar^2}{2\mu}\nabla^2 f_{\mathbf{k}} + \hbar\omega_l f_{\mathbf{k}} - \frac{\hbar^2}{2\mu}\nabla f_{\mathbf{k}} \cdot \frac{\nabla|\varphi|^2}{|\varphi|^2} = \rho_{\mathbf{k}} M_{\mathbf{k}} \tag{13}$$

can be solved exactly for fixed values of the parameters β and γ: the solutions are expressed in terms of the regular and irregular confluent hypergeometric functions [16–18]. Then the parameters β and γ of the pair envelope function are fixed, in a variational way, by imposing the total energy, ϵ_t, to be at a minimum. Since ϵ_t reduces to that of two free polarons in the LLP approximation [13] when the average distance between the particles is much larger than the polaron radius ($\gamma = \beta = 0$), the bipolaron binding energy is calculated subtracting from the total energy that of two LLP free polarons. In particular it has been shown that the bipolaron state exists only if the e-ph coupling constant α is greater than a critical value $\alpha_c = 6$ and when $\eta = \epsilon_\infty/\epsilon_0$ is smaller than a critical value $\eta_c = 0.01$ [16,17].

It is worth to note that in the intermediate coupling regime it is not possible to neglect the $f_{\mathbf{k}}$ dependence on r. In this case the phonons follow instantaneously the relative motion of the two electrons and, then, the wave function (10) contains, on average, the retardation effects of the e-e interaction mediated by the longitudinal optical phonons.

Within this variational approach it is possible to obtain an effective e-e potential due to the exchange of virtual phonons. In fact, the minimization procedure gives rise to two coupled differential equations for $f_{\mathbf{k}}$ and φ which are solved self-consistently. With the choice (12) for the envelope function it is possible, as mentioned, to solve exactly the differential equation for $f_{\mathbf{k}}$ as a function of the variational parameters β and γ. In the centre of mass frame the total energy minimization with respect to $\varphi(\mathbf{r})$, $\frac{\delta\langle\psi|H_1|\psi\rangle}{\delta\varphi}$, gives a Schrodinger-like equation for the two electrons from which it is possible to define an effective potential depending by β and γ known the functions $f_{\mathbf{k}}$ [18]:

$$v(r) = \frac{e^2}{\epsilon_\infty r} + \frac{\hbar^2}{2\mu}\sum_{\mathbf{k}} |\nabla f_{\mathbf{k}}|^2 + \sum_{\mathbf{k}} \left[\left(\frac{\hbar^2 |k|^2}{2M} + \hbar\omega_e\right)|f_{\mathbf{k}}|^2\right] - \sum_{\mathbf{k}} [\rho_{\mathbf{k}} M_k f_{\mathbf{k}} + c.c.] \ . \tag{14}$$

Typical effective potentials $v(r)$ are shown in Figure 1. They contain a short range attractive term and a long range repulsive term screened at large distances by the static dielectric constant ϵ_0 and, in the opposite limit, by the background high frequency dielectric constant ϵ_∞. It is worth to note that the proposed approach can be, in principle, improved if one chooses better and better estimate for the effective potential.

For the polar materials that are characterized by a value of α smaller than α_c, there is not bipolaron formation and the variational approach gives $\gamma = \beta = 0$. Consequently $v(r)$ coincides with the asymptotic effective e-e potential, *i.e.*, with the effective potential of two electrons whose relative average distance is much larger than the polaron radius. On the other hand, for $\alpha > \alpha_c$ the effective potential supports the bipolaron formation. However, it is worth to note that bipolaron formation in the limit of vanishing density does not imply the existence of bipolarons at finite densities.

The proposed procedure allows us to eliminate the phonon degrees of freedom from the system, simplifying the treatment of many electron effects, and to investigate larger values of the electron-phonon coupling constant with respect to the perturbative approach proposed by Mahan. This happens since the LLP transformation [13] gives rise to phonon corrections to the bare e-ph vertex [19], corrections which can be neglected according to the Migdal theorem [20] only when the Fermi energy is much larger than $\hbar\omega_l$ (normal metals).

As mentioned before our approach contains two main approximations: a) the e-e and e-ph interactions are not treated on the same footing; b) the variational effective potential which contains the e-ph effects is not ω-dependent as expected, for instance, in the usual Eliashberg theory of superconductivity [21]. However, these two approximations are not significant limitations for the physical situation which are aimed to describe. For low values of the electron density (low doping) and for both weak and intermediate e-ph interactions ($\alpha < 7$) it is clear that the approach is correct since the e-e effects are less important compared to the e-ph effects and the physics is controlled by the formation of polarons and, if it is possible, bipolarons well described by the LLP variational approach that we adopted. A mention deserves the strong e-ph coupling regime ($\alpha > 7$) [2]. Recently it has been shown [9], by using the path integral technique, that the Wigner crystallization of polarons is favoured with respect to the metallic state up to critical electron density, n_c, of the order of $n_c \sim 10^{19}$ cm^{-3}. For $n > n_c$ the system of dielectrics polarons cannot form a liquid state at zero temperature and

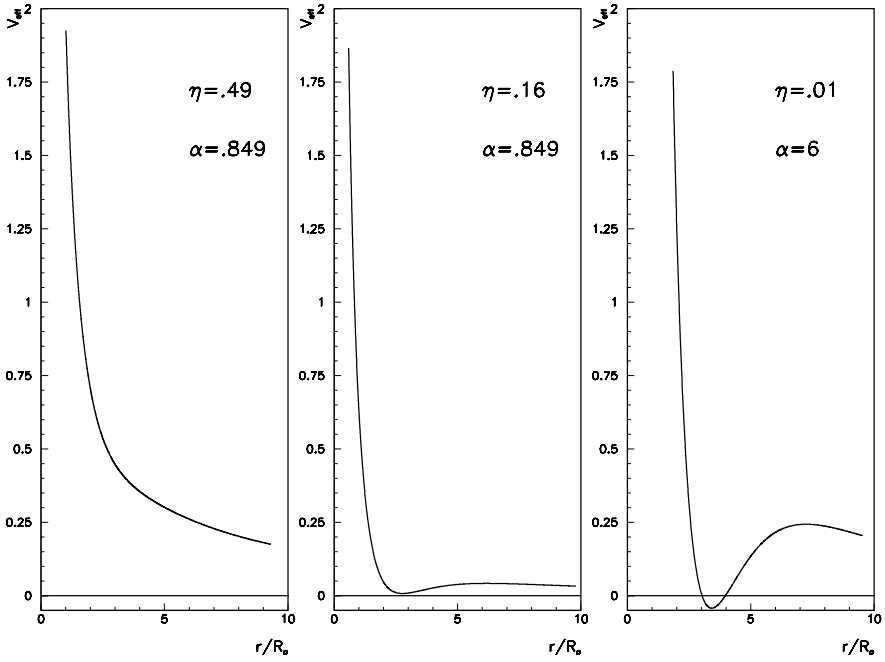

Fig. 1. The effective self-consistent electron-electron potential. The energies are given in units of $\hbar\omega_l$ and are measured from $-2\alpha\hbar\omega_l$. The parameters of Figure 1a correspond to the characteristic values of ZnO.

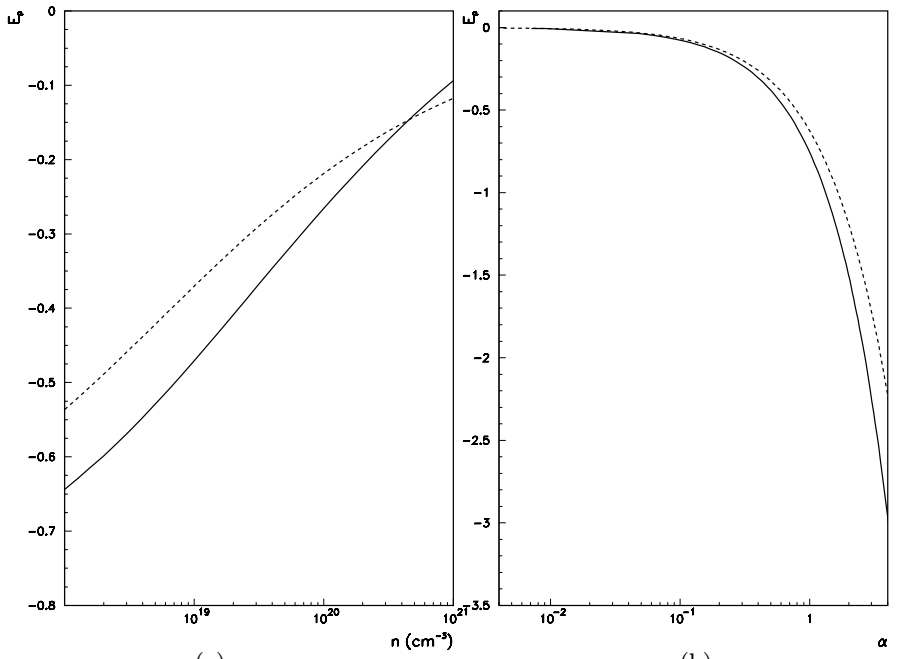

(a) (b)

Fig. 2. (a) Electron-phonon contribution to the ground state energy per particle in the variational (dotted line) and in our model (solid line) as a function of the electron density. The energies are given in units of $\hbar\omega_l$; (b) The same quantity is plotted for a fixed value of the electron density, $n = 10^{18}$ cm^{-3}, as a function of the e-ph coupling constant. The parameters are the same of ZnO, except ϵ_∞, that varies from 1.4 to 8.15.

the transition to the metallic phase is driven by the polaron dissociation. In this work the regime characterised by very strong e-ph interactions will not be analyzed.

The regime of larger doping but still such that ($\omega_p^0 < \omega_l$, ω_p^0 being the plasma frequency screened by ϵ_0) and weak e-ph interaction also does not present any problem; in fact, as we will discuss later, our approach is equivalent to the available theories that do not suffer from the restrictions due to the approximations a) and b).

The validity of our approach is less evident for intermediate e-ph interaction and $\omega_p^0 \sim \omega_l$. In fact, it is well-known that the electron corrections to the bare e-ph vertex tend to suppress the effective phonon-mediated e-e interaction when $v_F q/\omega \gg 1$, q and ω being the transferred momentum and energy. As a consequence, our approach should overestimate e-ph effects unless ω is very large. However, when the system is close to a charge-density waves instability, it has been shown that the vertex corrections due to the e-e repulsion are ineffective also in the limit $v_F q/\omega \gg 1$, while the phonon vertex corrections are particularly relevant [14]. In other words, it is a reasonable approximation to treat first the phonon corrections to the e-ph vertex and then to consider the effects due to the presence of many electrons. This recovers the validity of our approach.

Finally we note that at very large values of the carrier density, typical of the ordinary metals, the proposed approach is not able to describe the physics correctly since the retardation effects of the effective phonon-mediated e-e are relevant, electron screening very effective and the phonon vertex corrections are negligible according to the Migdal theorem [20].

The model proposed is studied within the RPA [22] and Hubbard approximation [23] at $T = 0$. Within these approximations the effective interaction between the electrons takes the form:

$$V_{eff}(q,\omega) = \frac{v(q)}{1 - V^*(q,\omega)/[1 + f(q)V^*(q,\omega)]} = \frac{v(q)}{\epsilon(q,\omega)} \tag{15}$$

where $V^*(q,\omega) = v(q)\Pi^0(q,\omega)$ and $\Pi^0(q,\omega)$ is the lowest order proper polarization propagator. The function $f(q)$ takes the value 0 in the RPA [22] and

$$f(q) = \frac{1}{2}\frac{v\left(\sqrt{q^2 + q_F^2}\right)}{v(q)} \tag{16}$$

in the Hubbard approximation [23]. The RPA excluding exchange diagrams overestimates the contribution of the short range terms by around a factor of two. The Hubbard approximation takes into account approximatively these terms making an estimate of the contribution of all proper polarization insertions with repeated horizontal interaction lines across the fermion loop. In the limit of large electron densities the Hubbard approximation coincides with the RPA, the dominant contribution to the correlation energy coming from low momentum transfers.

The calculation of the self-energy to the lowest order in the dynamically screened interaction $V_{eff}(q,\omega)$ gives:

$$\Sigma(k,\omega) = \frac{i}{\hbar\,(2\pi)^4} \times \int_{-\infty}^{\infty} d\omega_1 \int d\mathbf{q}\;\; G^0(\mathbf{k}-\mathbf{q}, \omega-\omega_1)\frac{v(q)}{\epsilon(q,\omega_1)} \tag{17}$$

where $G^0(q,\omega)$ is the propagator for non interacting electrons [24]

$$G^0(q,\omega) = \frac{\Theta(q-q_F)}{\omega - E_q^0/\hbar - \epsilon_0^* + i\eta} + \frac{\Theta(q_F - q)}{\omega - E_q^0/\hbar - \epsilon_0^* - i\eta}\,. \tag{18}$$

In the following we will focus our attention on the properties of the normal state: therefore the energy shift ϵ_0^* is chosen so that the chemical potential of the non interacting system $\mu = \hbar^2 k_F^2/2m + \epsilon_0^*$ coincides with that obtained by the equation [25,26]:

$$\mu = \frac{\hbar^2 k_F^2}{2m} + \Sigma(k_F, \mu - \epsilon_0^*). \tag{19}$$

Equation (19) combined with the above expression for μ gives:

$$\epsilon_0^* = \Sigma(k_F, \frac{\hbar^2 k_F^2}{2m})\,. \tag{20}$$

Finally to evaluate the self-energy we follow the treatment proposed by Quinn and Ferrel [27], which retains all contributions coming from the continuum of the electron-hole pair states.

3 Weak coupling

The aim of this section is to compare a number of properties, obtained within the model introduced before, with the results given by the variational and perturbative approaches. In particular we will focus our attention on the total energy, the collective excitations and the single-particle self-energy: numerical results will be presented for ZnO, which is characterised by the following parameters [28]: $m = 0.24 m_e$, $\epsilon_\infty = 4$, $\epsilon_0 = 8.15$, $\hbar\omega_l = 73.27$ meV, $\alpha = 0.849$.

3.1 The total ground state energy

The total ground state energy per particle takes the following form:

$$E_T = T_0 + E_{ex} + E_{corr} \tag{21}$$

where

$$
\begin{aligned}
T_0 &= \frac{3}{5}E_F \\
E_{ex} &= -\frac{Vk_F^3}{12N\pi^4} \\
&\quad \times \int_0^{2k_F} dq\, q^2 v(q) \left[1 - 1.5\frac{q}{2k_F} + 0.5\left(\frac{q}{2k_F}\right)^3\right] \\
E_{corr} &= \frac{3e^2}{4a_B\pi\alpha_1^2 r_s^2}\int_0^\infty dq\,\frac{q^2}{2k_F^3}\int_0^\infty \frac{d\omega}{2E_F} \\
&\quad \times \left[\frac{1}{g(q)}\arctan\left(\frac{v(q)\mathrm{Im}\Pi^0(q,\omega)g(q)}{1-g(q)v(q)\mathrm{Re}\Pi^0(q,\omega)}\right)\right. \\
&\quad \left. -v(q)\mathrm{Im}\Pi^0(q,\omega)\right] \\
\alpha_1 &= \left(\frac{4}{9\pi}\right)^{1/3} \\
g(q) &= 1 - f(q). \qquad (22)
\end{aligned}
$$

In equation (21) T_0 and E_{ex} are the kinetic and potential energy, respectively, in HF approximation; E_{corr} is the correlation energy in the Hubbard approximation and r_s is the radius, in the Bohr units, of a sphere whose volume is equal to the volume per particle. In particular in the limit $\epsilon_0 = \epsilon_\infty$ and $m = m_e$ equation (21) provides the total ground state energy per particle of a Coulomb gas. In Figure 2a the contribution of the e-ph interaction to the ground state energy in the variational [29] and our approaches are plotted as a function of the electron density. In the variational approach this contribution is given by E_p in equation (3). Since in our model it is not possible to express the total ground state energy as the sum of two independent terms, the e-ph contribution to E_T is obtained subtracting from E_T the energy per particle of a Coulomb gas screened by the background high frequency dielectric constant ϵ_∞. In both models, increasing the density, $|E_p|$ decreases, the screening of the Coulomb gas on the polaron self-energy becoming bigger and bigger. However, in our approach the effect of the electron screening is slightly less effective for low values of the doping. Instead, for very large electron densities, our model underestimates the effects of the e-ph interaction. In Figure 2b the same quantity is plotted as a function of α for a fixed value of the electron density, $n = 10^{18}$ cm^{-3}. It is evident that the two approaches provide the same results when the e-ph coupling constant is very little ($\alpha < 1$).

3.2 Collective excitation spectrum

The collective excitation frequencies of the system are determined by the poles of the retarded density correlation function, which occur at the solutions $\Omega_q - i\gamma_q$ of the equation:

$$\epsilon^R(q, \Omega_q - i\gamma_q) = 0. \qquad (23)$$

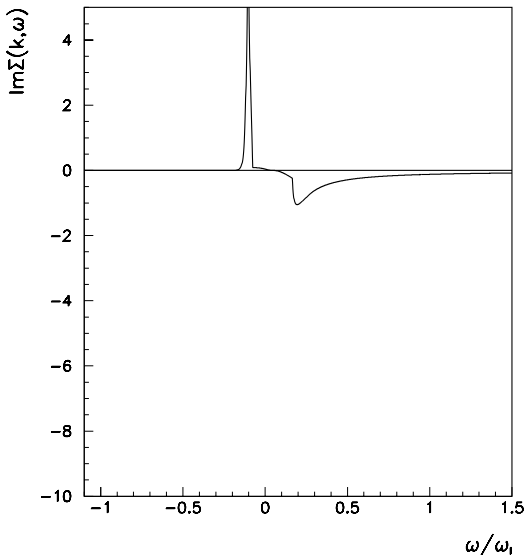

Fig. 3. The imaginary part of the self energy for $k = 0.5k_F$ as a function of the electron energy $\hbar\omega$ measured from ϵ_0^* at $n = 10^{17}$ cm^{-3}. Im$\Sigma(k,\omega)$ is given in units of $4E_F$.

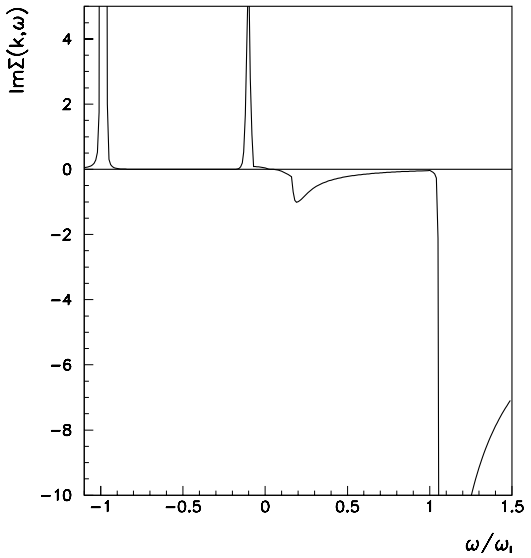

Fig. 4. The imaginary part of the self energy for $k = 0.5k_F$ as a function of the electron energy $\hbar\omega$ measured from ϵ_0^* at $n = 10^{17}$ cm^{-3} in the perturbative approach. In the region of the characteristic polaronic energies these results are very similar to that obtained in our model reported in Figure 3. Im$\Sigma(k,\omega)$ is given in units of $4E_F$.

In the perturbative approach the dielectric function is chosen to be the sum of three contributions [5]:

$$\epsilon(q,\omega) = \epsilon_\infty + \frac{\epsilon_0 - \epsilon_\infty}{1 - \omega^2/\omega_T^2} - v_q^\infty \Pi^0(q,\omega) \qquad (24)$$

where ω_T is the transverse optical phonon frequency. This expression, which is exact within the RPA, takes into

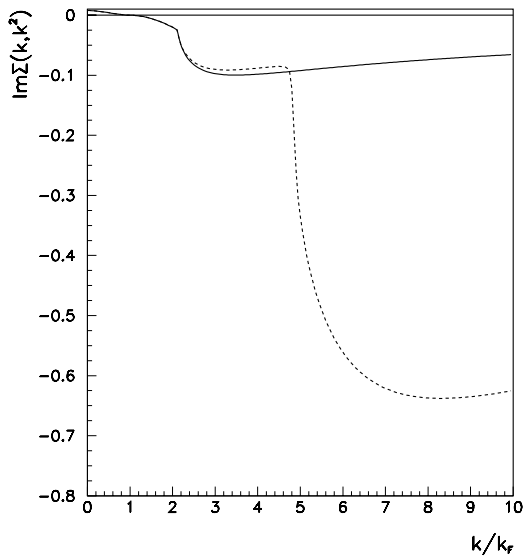

Fig. 5. The imaginary part of the quasi-particle self energy $\mathrm{Im}\Sigma(k,k^2)$ as a function of the momentum k of the electron at $n = 10^{17}$ cm^{-3} in our model (solid line) and in the perturbative approach (dotted line). The energies are given in units of $\hbar\omega_l$.

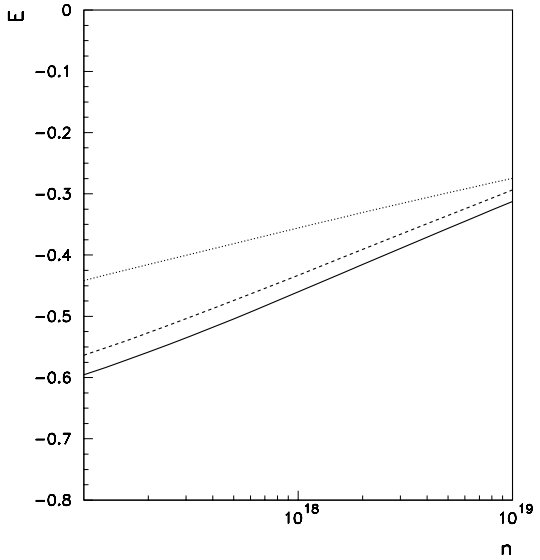

Fig. 6. The contribution of the electron-phonon interaction to the correction of the band edge in the perturbative approach making use of the RPA (solid line), static RPA (dashed line) and Thomas-Fermi (dotted line) approximations as a function of the electron density. The energies are given in units of $\hbar\omega_l$.

account the screening effects due to the electron gas, the optical phonons and the high energy electronic excitations. Equation (24) is a quadratic equation for ω^2 in the limit $q \to 0$: therefore there are always two roots $\omega_1^2(q)$ and $\omega_2^2(q)$ that are a mixing of the phonon and plasmon excitations. There are two opposite limits in which the many-polaron effects can be easily treated: they occur when the plasma frequency ω_p^∞ (the plasma frequency screened by ϵ_∞) is much smaller or much larger than ω_l.

In the former case ω_1 tends to ω_l, the electron gas being not able to oscillate as fast as the phonons. On the other hand, since the phonons can follow the motion of the electrons $\omega_2(q=0)$ tends to the plasmon frequency screened by ϵ_0. The situation is different when ω_p^∞ is much larger ω_l. In fact the electrons see the ionic motion as static so that the static electron screening can be used. In this case the frequencies $\omega_1(q)$ and $\omega_2(q)$ have a different behaviour depending on the q value. In fact the electron gas has a characteristic screening length q_{TF}^{-1}, q_{TF} being the Thomas-Fermi wave vector, and the electron-electron interaction declines rapidly at distances larger than the screening length, thus for $q > q_{TF}$ the screening of the electron gas becomes less effective. For $q \ll q_{TF}$ the mode $\omega_2^2(q)$ tends to ω_T^2 while at large values of q it goes to ω_l^2 since the electron gas is not any longer able to screen the electron-phonon interaction. The phonons cannot follow the plasma oscillations of the electron gas: then the plasma frequency is screened by the dielectric constant ϵ_∞.

In our approach the description of the collective excitation spectrum is less rich. In fact since the retardation effects of the LO phonon-mediated e-e interaction have been neglected, there is always only one solution to equation (23). The collective excitation energy goes from $\hbar\omega_p/\sqrt{\epsilon_0}$ for $q \to 0$ to the roots of an electron gas screened by the background high frequency dielectric constant ϵ_∞ for large values of q. Particularly at low values of the electron density this mode coincides with the plasmon like mode in the perturbative approach. We also note that, in our approach, it is not possible to divide the dielectric function into different contributions due to the e-e interaction and e-ph interaction.

3.3 Imaginary part of the self-energy

In Figure 3 we show the results of the imaginary part of the electron self-energy $\mathrm{Im}\Sigma(k,\omega)$ in our model, as a function of ω in the Hubbard approximation. $\mathrm{Im}\Sigma(k,\omega)$ is zero for all k at $\hbar\omega = E_F$: a change of sign must occur at this point since the damping of electrons and holes is opposite in sign. The large peak contribution to $\mathrm{Im}\Sigma(k,\omega)$ is due to the excitation of the collective mode. Since the real and imaginary parts of $\Sigma(k,\omega)$ obey the Kramers-Kronigh dispersion relation, there is a corresponding structure in $\mathrm{Re}\Sigma(k,\omega)$: it has a finite discontinuity at the same point in which $\mathrm{Im}\Sigma(k,\omega)$ shows a peak. The other contribution to $\mathrm{Im}\Sigma(k,\omega)$ arises from the region where $\epsilon_2(k,\omega)$ is not zero, $\epsilon_2(k,\omega)$ being the imaginary part of the dielectric function, and it is due to the creation of particle-hole pairs. It is also possible to evaluate the imaginary part of the self-energy in the perturbative approach in which the effective potential between the electrons is the sum of a) the screened coulomb interaction and b) the screened electron-phonon interaction. The b) contribution is expressed as the product of the screened matrix element $M_q^2/(\epsilon_{el}^2(q,\omega))$ and

the phonon Green's function $D(q,\omega)$:

$$D(q,\omega) = \frac{D^0(q,\omega)}{1 - M_q^2 D^0 \Pi^0/\epsilon_{el}(q,\omega)} \tag{25}$$

where

$$\epsilon_{el}(q,\omega) = 1 - v_q^\infty \Pi^0(q,\omega)\ . \tag{26}$$

Mahan has calculated the one-phonon self-energy term from the electron-phonon interaction replacing the phonon Green's function $D(q,\omega)$ by the unperturbated propagator $D^0(q,\omega)$ and making use of the static dielectric function of Thomas-Fermi. The result is that $\mathrm{Im}\Sigma(k,\omega)$ is zero for energies within ω_l around the Fermi energy. The onset of $\mathrm{Im}\Sigma(k,\omega)$ for $\omega > \omega_l$ corresponds to the fact that the phonon emission processes are not possible until the energy is equal or greater than the phonon frequency ω_l. Moreover at $T = 0$, if the system is in equilibrium, the contribution to the imaginary part of the self-energy from the electron-phonon interaction becomes again zero for $\hbar\omega < -\hbar\omega_l - E_F$. The onset of $\mathrm{Im}\Sigma(k,\omega)$ at $\hbar\omega = -\hbar\omega_l - E_F$ corresponds to the process in which the electron with energy $-E_F$, jumps in the hole having energy $-\hbar\omega_l - E_F$. These results were first obtained by Engelsberg and Schrieffer [30] who considered a system of electrons coupled with the acoustical phonons. We have calculated the self-energy within the perturbative approach making use of the RPA approximation and the results are presented in Figure 4: besides the peak, due to the excitation of the coupled phonon-plasmon collective mode, the imaginary part of the electron self-energy shows a strong variation in the points $+\hbar\omega_l$, $-\hbar\omega_l$ and $-\hbar\omega_l - E_F$, but the amplitude of the gap coincides with that obtained making use of the Thomas-Fermi approximation for the dielectric constant only in the limit $\omega_p^\infty \gg \omega_l$. These results show, as it is reasonable, that the static approximation provides a good treatment of the electronic effects only when the plasma frequency is much larger than the characteristic phonon energies. Similar results have been obtained by Das Sarma *et al.* [31] who have calculated the quasi-particle damping rate which is proportional to the quantity $\Gamma(k) = \mathrm{Im}\Sigma(k,k^2)$. They showed that the static screening is a good approximation at very high electron densities, whereas the dynamically screened decay rate lies intermediate between statically screened and unscreened results. In Figure 5 $\Gamma(k)$ is plotted as function of k for the ZnO at $n = 10^{17}$ cm^{-3} ($\omega_p^\infty \ll \omega_l$), both in our model and in the perturbative approach making use of the RPA. In particular in the region close to the Fermi surface the damping rate goes like $\left(E^0(k) - \mu\right)^2$ where $E^0(k)$ is the quasi-particle energy: this is a simple consequence of the Pauli principle restrictions. The peaks in $\Gamma(k)$ are caused by processes corresponding to the excitations of the two renormalized modes $\omega_1(k)$ and $\omega_2(k)$. Moreover it is evident that at low electron densities $\omega_p^\infty \ll \omega_l$ our model neglects, with respect to the perturbative approach, excitation processes involving high energy, whereas it provides a good treatment of the characteristic polaronic energies. We draw the same conclusions evaluating the polaronic corrections to the band edge which, in the Rayleigh-Schrodinger perturbation theory, are given by $E_p = \mathrm{Re}\Sigma_1(k=0,\omega=0)$, $\Sigma_1(k,\omega)$ being the one-phonon self-energy term from the e-ph interaction. In Figure 6 we present the results for E_p in the perturbative approach making use of the RPA, static RPA and the Thomas-Fermi approximations. It is clear that the Thomas-Fermi approximation overestimates the screening effects at low densities, giving a smaller polaronic binding energy than the dynamically screened results. In the opposite limit, instead, the two approximations provide the same results.

3.4 The spectral weight function

The spectral weight function is the imaginary part of the electron propagator and therefore it can be expressed in term of the real and imaginary parts of the self energy $\Sigma_{ret}(k,\omega)$ [36]

$$A(k,\omega) = -\frac{2\mathrm{Im}\Sigma_{ret}(k,\omega)}{\left[\omega - E_k^0/\hbar - \mathrm{Re}\Sigma_{ret}(k,\omega)\right]^2 + \left[\mathrm{Im}\Sigma_{ret}(k,\omega)\right]^2}\ . \tag{27}$$

Figures 7a and 7c show $A(k,\omega)$ in the Hubbard approximation for two different values of η. The energy $E(k)$ and the damping rate $\Gamma(k)$ of a quasi-electron ($k > k_F$) and a quasi-hole ($k < k_F$) are the poles of the analytic continuation of $G(k,\omega)$ into the lower right and upper left half plane for ω:

$$E(k) = \frac{\hbar^2 k^2}{2m} + \mathrm{Re}\Sigma\left(k, \frac{E(k) + i\Gamma(k)}{\hbar}\right) \tag{28}$$

and

$$\Gamma(k) = \mathrm{Im}\Sigma\left(k, \frac{E(k) + i\Gamma(k)}{\hbar}\right)\ . \tag{29}$$

In particular for long lived single particle excitations the energy $E(k)$ and the damping rate $\Gamma(k)$ are given by:

$$E(k) = \frac{\hbar^2 k^2}{2m} + \mathrm{Re}\Sigma\left(k, \frac{E(k)}{\hbar}\right) \tag{30}$$

and

$$\Gamma(k) = \frac{\mathrm{Im}\Sigma(k, \frac{E(k)}{\hbar})}{\left(1 - \frac{\partial \mathrm{Re}\Sigma(k,\omega)}{\partial\omega}\right)\Big|_{\frac{E(k)}{\hbar}}}\ . \tag{31}$$

The numerical solution of equation (30) shows the existence of three roots. The one at highest energy is the regular quasi-particle solution (screened polaron), which is very little shifted from the Hartree-Fock value. It describes electrons surrounded by a dynamic polarization cloud due to the effective e-e interaction: the self-energy

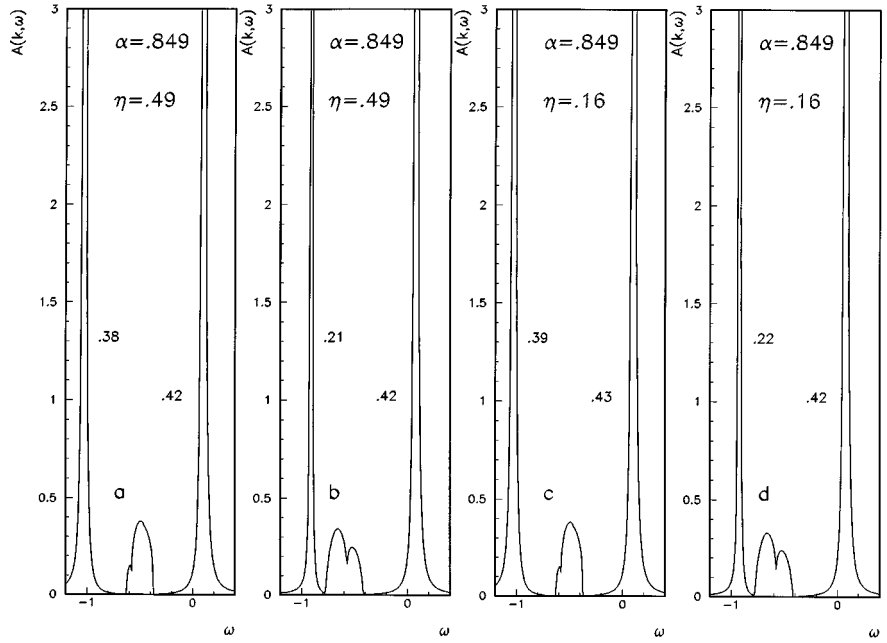

Fig. 7. The one-particle spectral function in the range of the characteristic polaronic energies for $k = 0.5k_F$ and at $n = 10^{17}$ cm^{-3}, in our model and in the perturbative approach for two different values of η (a, c and b, d respectively). In both cases ϵ_0^* is of order of $\epsilon_0^* \sim -\alpha\hbar\omega_l$. The energies are given in units of $4E_F$. The parameters of Figures 7a and 7c correspond to the characteristic values of ZnO. The spectral weights relative to the different peaks are indicated.

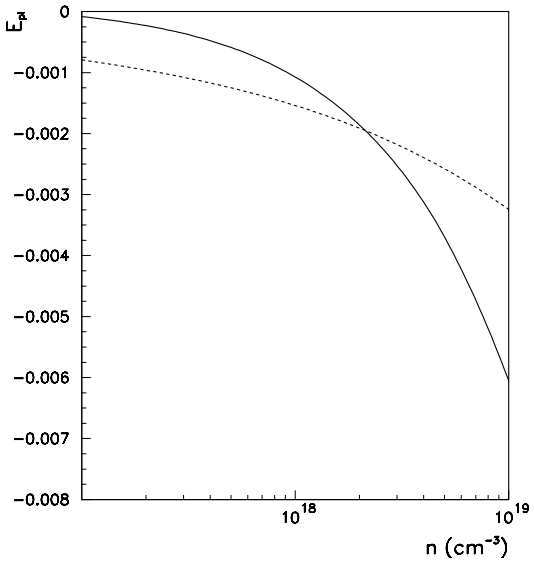

Fig. 8. The plasmapolaron self-energy as a function of the electron density in our model (solid line) compared with that obtained in reference [37]. The energies are given in Ry and are measured from $-\alpha\hbar\omega_l$.

at $q = 0$ of this quasi-particle increases with the particle density. Another solution appears at the finite discontinuity of $\mathrm{Re}\Sigma(k,\omega)$ and it doesn't give contribution to the spectral weight function having the imaginary part of the electron self-energy a peak at the same energy. To understand the physical meaning of the other solution it is convenient to separate the contribution of the exchange term from the self-energy: $\Sigma(k,\omega) = \Sigma_{exc}(k,\omega) + \Sigma^*(k,\omega)$. The contribution given by $\Sigma^*(k,\omega)$ can be viewed as that of a particle coupled to the density fluctuations propagator $S(k,\omega)$, whose spectral representation is:

$$S(k,\omega) = -\frac{1}{\pi v(k)} \int_0^\infty d\omega_1 \mathrm{Im} \frac{1}{\epsilon(k,\omega_1)} \frac{2\omega_1}{\omega^2 - (\omega_1 - i\delta)^2} \cdot \tag{32}$$

On the other hand, the single-particle self-energy of a fermion coupled to a boson field with the Bose propagator:

$$D(k,\omega) = \frac{2\omega(k)}{\omega^2 - \omega^2(k) + i\delta} \tag{33}$$

and the effective coupling:

$$g^2(k) = \frac{v(k)}{\left|\frac{\partial\epsilon(k,\omega)}{\partial\omega}\right|_{\omega(k)}} \tag{34}$$

takes exactly the form $\Sigma^*(k,\omega)$ if the further approximation of single plasma pole for the density fluctuations $S(k,\omega)$ is used [26]. Therefore $\Sigma^*(k,\omega)$ can be approximately described as the contribution of a particle interacting with a boson field: the plasmon-phonon. The quasi-particle formed by an electron surrounded by a cloud of virtual excitations (plasmon-phonon) is usually called plasmapolaron [37].

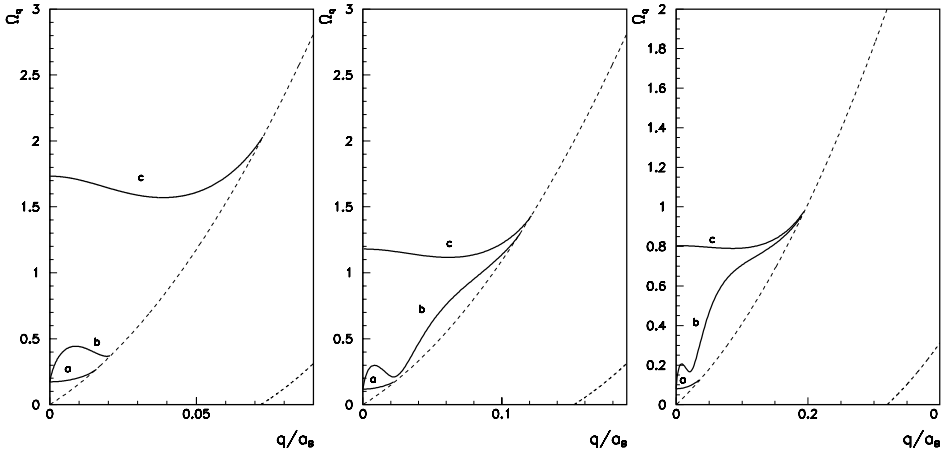

Fig. 9. The curves (a) and (c) represent the collective excitation spectrum of the Coulomb gas screened by ϵ_0 and ϵ_∞ respectively at different electron densities ($n = 10^{19}$ cm^{-3}, $n = 10^{20}$ cm^{-3}, $n = 10^{21}$ cm^{-3}). The particle-hole excitations lie between the dotted lines. The curve (b) represents the energy of the collective mode as a function of the wave vector q using the potential plotted in Figure 1. The energies $\hbar\Omega(q)$ are given in units of $4E_F$.

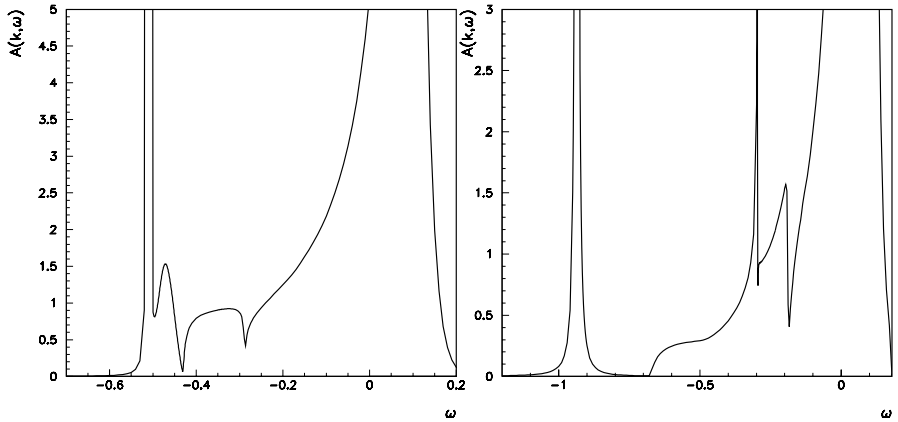

Fig. 10. The one-particle spectral function for $k = 0.01k_F$ as a function of the electron energy at different charge carrier densities ($n = 10^{19}$ cm^{-3}, $n = 10^{20}$ cm^{-3}). The energies are given in units of $4E_F$.

The quantity $E - \epsilon^*_{0r}$, where E is the $q = 0$ self-energy of the plasmapolaron, *i.e.* the solution of the equation $E = \mathrm{Re}\Sigma(0, E)$, and ϵ^*_{0r} is the shift in the chemical potential for a Coulomb gas screened by ϵ_∞, is plotted as a function of the electron density in Figure 8. It is in good agreement with that calculated starting by the Hamiltonian of an electron interacting with the phonon and plasmon boson fields and using a variational approach based on the LLP transformation [37]. The differences between the two plots are due to the presence, in the self-energy, of the continuum of the electron-hole pair states, exchange and correlation terms. These contributions are not considered in the variational approach proposed in reference [37].

In Figures 7b and 7d the spectral weight function in the perturbative approach is plotted for the same values of η, n and k. It is well-known that, in the perturbative approach, $A(k, \omega)$ for a single electron coupled to the longitudinal optical phonons shows, at $T = 0$ and for $k = 0$, a delta-function peak and an incoherent contribution, with very small spectral weight, which starts at $\omega = \omega_l$ [5]. The effect of the e-e interaction is to split the single delta-function peak in two lorentian functions that describe two quasi-particle: the polaron and the plasmapolaron. The comparison between Figures 7a and 7b points out, again, that our approach takes well into account the characteristic polaronic energies and neglects the excitation processes involving high energies ($\omega > \omega_l$). This is a reasonable approximation when $\omega_p^0 < \omega_l$.

It is worth to note that, increasing the charge carrier density, the polaron, an electron dressed by a cloud of virtual phonons, evolves towards a new quasiparticle, an electron weakly renormalized by the scattering with the phonons, *i.e.*, a quasiparticle with reduced energy and mass with respect to the values $E_p(q = 0) = -\alpha\hbar\omega_l$ and

$m^* = m/(1-\alpha/6)$. Instead the plasmapolaron evolves towards an electron dressed by a cloud of virtual plasmons.

4 Intermediate coupling ($\alpha \sim \alpha_c$)

4.1 Collective excitation spectrum

It is well-known that the retarded dielectric function is analytic in the upper half of the complex plane provided [32] $\epsilon^R(k,0) \geq 0$. There are examples of physical systems for which the linear response function violates the causal requirement: in this case the linear retarded dielectric function can no longer describe the behaviour of the system correctly. It has been shown that the temperature dependent correlation function in the RPA for an interacting many-particle system, $\epsilon^R(k,\omega)$, when the interaction is sufficiently attractive, has forbidden zeros on the imaginary axis of the complex frequency plane [33]. These poles of the linear response function appear even in the classical limit where they correspond to the transition of the system from a gaseous to a liquid state. A similar situation is found in the case of a superconductor [34]. While in the perturbative approach the causal requirement is never violated, even if the interaction electron-phonon is extremely strong, in our model, if the value of the coupling constant α is sufficiently large, the linear response function possesses a pair of imaginary poles. It is interesting to note that the same type of instability has been suggested by Di Castro *et al.* for a large class of systems of interacting electrons and phonons as due to very ineffective electron corrections to the e-ph vertex [14].

The results which will be shown here and in the following subsections have been obtained choosing the model parameters in such a way the system is just above the appearance of the instability. The parameters chosen are: $m = m_e$, $\eta = 0.01$, $R_p = 10$ Å, $\alpha\hbar\omega = 0.016\ Ry$, $(\alpha \sim \alpha_c)$.

In Figure 9 we present the numerical results for the collective excitation spectrum in the Hubbard approximation. The collective mode energy softens for a critical wave vector q indicating strong correlation between the electrons. If the attractive potential is sufficiently strong the collective energy softens completely. This softening, present in a finite range of densities $10^{19} - 10^{21}$ cm^{-3}, means that the system becomes unstable with respect to the formation of the charge density waves. Similar results are also obtained in the Hubbard model with on site attraction [35] and using the slave-boson approach for the infinite U three band Hubbard model [14].

4.2 The spectral weight function

Figure 10 shows $A(k,\omega)$ for $k = 0.01k_F$ and for different values of the electron density in the Hubbard approximation. Beside the peaks already present in the weak coupling regime the equation (30) exhibits a new solution with energy between the plasmapolaron and quasi-particle branches. It appears only if the strength of the attractive potential is sufficiently large and the damping rate of this excitation increases very quickly as a function of k. Then it exists as a well-defined excitation of the system only for moments well inside the Fermi surface. As mentioned before this excitation is related to the attractive part of the potential and it is present only close to the instability signaled by the complete softening of the collective mode energy. This interpretation is also confirmed by the behaviour of the renormalization coefficient of the one-electron Green's function:

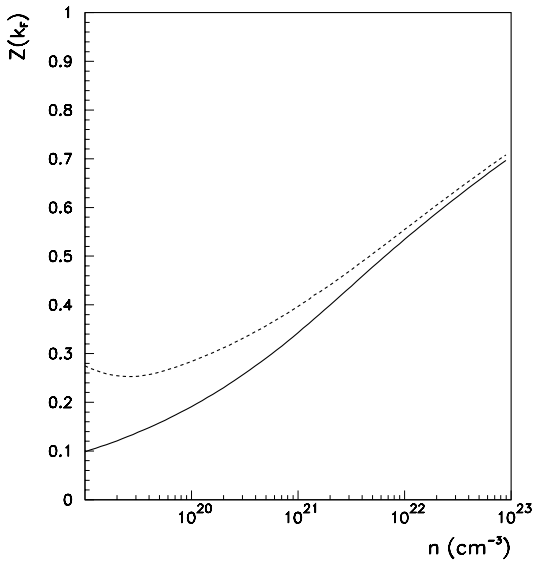

Fig. 11. The renormalization coefficient of the one-electron Green's function at $k = k_F$ as a function of the density. The solid line represents $Z(k_F)$ for a Coulomb gas screened by the background high frequency dielectric constant ϵ_∞.

$$Z(k) = \frac{1}{1 - \dfrac{\partial \mathrm{Re}\Sigma(k,\omega)}{\partial\omega}}\,. \tag{35}$$

At $k = k_F$, $Z(k_F)$ is the magnitude of the discontinuity at $k = k_F$ in the momentum distribution $n(k)$ [38]. In Figure 11 $Z(k_F)$ is plotted as a function of the electron density and it is compared with the renormalization coefficient of a Coulomb gas screened by the background high frequency dielectric constant ϵ_∞ [39]. In the range of densities in which the new elementary excitation appears, $Z(k_F)$ has a minimum; increasing the electron density it tends to the value of a Coulomb gas screened by ϵ_∞. These results indicate that the charge density wave instability is a source of a strong quasi-particle scattering and suggest that the new peak in the spectral weight function could be a metastable double occupied state (bipolaron).

4.3 The dispersion curves

We end this section showing the dispersion curves of the three excitations $E_i(k)$ in the region of k in which the decay is due only to the excitations of particle-hole pairs

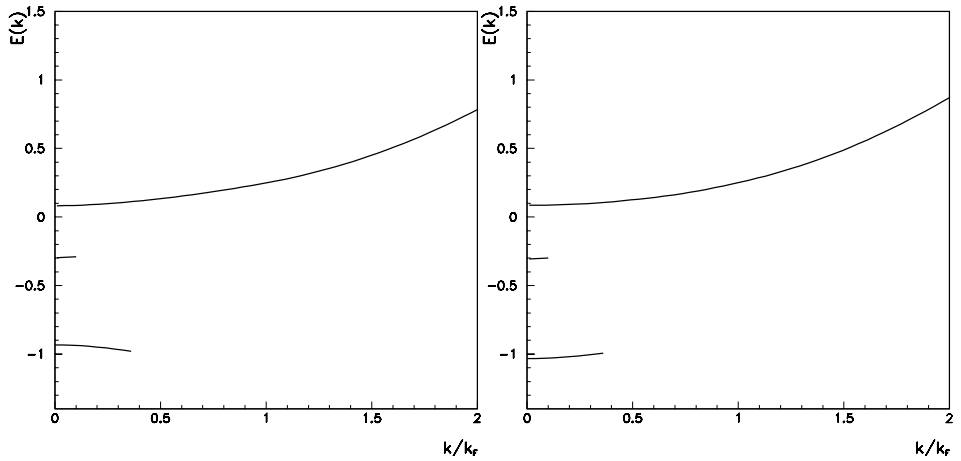

Fig. 12. The dispersion curves at different electron densities ($n = 10^{20}$ cm^{-3}, $n = 10^{21}$ cm^{-3}) in the region of k in which the decay is due only to the particle-hole pairs excitations. The energies are given in units of $4E_F$.

(Fig. 12). They have been obtained following the poles of the analytic continuation of $G(k, \omega)$. In particular, for k less than k_F and energies less than μ, these poles describe the state obtained by creating a hole in the interacting ground state. The curves $E_i(k)$ are drawn only for k values which do not involve the creation of collective excitations. In fact the decay for the quasi-particle band due to the creation of collective excitations starts for a value of the electron momentum which satisfies the conservation of the energy:

$$\frac{\hbar^2 k^2}{2m} = \frac{\hbar^2 k_F^2}{2m} + \hbar\omega(k - k_F) \tag{36}$$

$\omega(k)$ being the collective excitation spectrum of the system, while the critical momentum which characterizes the decay of a plasmapolaron is given by the condition:

$$E(k) - \mu < -\hbar\omega(k + k_F) \ . \tag{37}$$

Both the quasi-particle and plasmapolaron have approximatively quadratic dispersion laws.

5 Conclusions

A model for an interacting gas of large polarons has been introduced. In the model the electrons interact each other with a non retarded effective potential obtained within a variational approach [16] valid for large polarons in the intermediate e-ph coupling. The effective potential is able to recover the large polaron properties in the limit of zero density. Then the many-body problem has been studied within the RPA and Hubbard approximations. The ground state energy, the single-particle self-energy and the collective excitation spectrum for a system of interacting large polarons have been calculated at densities typical of the metallic phase of doped polar semiconductors and doped perovskites. The numerical results have been compared with those provided by two traditional approaches in which the e-e and e-ph interactions are taken into account at the same level. It has been shown that the polaron self-energy is strongly reduced compared to that obtained in the zero density limit. For intermediate values of the e-ph coupling constant the collective mode energy presents a softening in a finite range of densities at a finite value of q signaling a CDW instability as suggested in recent works about the e-ph interaction in presence of strong correlations [14] and the single-particle spectrum shows a new elementary excitation, a bipolaronic metastable state, with energy between the plasmapolaron and the quasi-particle branches.

The authors are grateful to Prof. M. Marinaro for interesting discussions during the course of this work. GDF also thanks the European Economic Community for financial support.

References

1. L. Landau, Phys. Z. Sowjetunion **3**, 664 (1933); English translation, *Collected Papers* (Gordon and Breach, New York, 1965), pp. 67-68.
2. S.I. Pekar, *Research in Electron, Theory of Crystals* (Gostekhizdat, Moscow, 1951); English translation: *Research in Electron Theory of Crystals*, US AEC Report AEC-tr-5575 (1963).
3. H. Fröhlich, *et al.*, Philos. Mag. **41**, 221 (1950); H. Fröhlich, in *Polarons and Excitons*, edited by C.G. Kuper, G.A. Whitfield (Oliver and Boyd, Edinburg, 1963), p. 1.
4. J.T. Devreese, Polarons, in: *Encyclopedia of Applied physics*, edited by G.L. Trigg (VCH, New York, 1996) and references therein.
5. G.D. Mahan, *Many-Particle physics* (Plenum, New York, 1981), Chap. 6; G.D. Mahan, in *Polarons in Ionic Crystals and Polar Semiconductors* (North-Holland, Amsterdam, 1972), p. 553.
6. A.A Shanenko, M.A. Smondyrev, J.T. Devreese, Solid State Commun. **98**, 1091 (1996).

7. D. Emin, Phys. Rev. B **45**, 5525 (1992); Phys. Rev. Lett. **62**, 1544 (1989).
8. M. Capizzi, *et al.*, Phys. Scr. T **66**, 215 (1996) and references therein.
9. P. Quemerais, S. Fratini, Mod. Phys. Lett. B **9**, 25 1665 (1995); P. Quemerais, S. Fratini, Mod. Phys. Lett. B **11**, 30, 1303 (1997), cond-mat/9709182.
10. G.D. Mahan, C.B. Duke, Phys. Rev. **149**, 705 (1966).
11. In the polar semiconductors and perovskites the value of the parameter r_s (the radius of a sphere equal in volume to the volume per electron in units of the Bohr radius) has to be calculated, in the weak and intermediate e-ph coupling regime, using the effective Bohr radius which contains the static dielectric constant and the effective mass of the electrons in the conduction band. In these compounds the effective Bohr radius may be around 50 Å so that even for an electron density around $n = 10^{17}$ cm^{-3} the value of r_s is around one: this justifies the use of RPA and Hubbard approximations.
12. L.F. Lemmens, J.T. Devreese, F. Brosens, Phys. Status Solidi B **82**, 439 (1977).
13. T.D. Lee, F. Low, D. Pines, Phys. Rev. **90**, 297 (1953).
14. M. Grilli, C. Castellani, Phys. Rev. B **50**, 16880 (1994); C. Castellani, C. Di Castro, M. Grilli, J. Supercond. **9**, 413 (1996); C. Castellani, C. Di Castro, M. Grilli, Phys. Rev. Lett. **25**, 4650 (1995).
15. V.J. Emery, S.A. Kivelson, Physica C **209**, 597 (1993); V.J. Emery, S.A. Kivelson, Physica C **235-240**, 189 (1994).
16. V. Cataudella, G. Iadonisi, D. Ninno, Phys. Scr. T **39**, 71 (1991).
17. F. Bassani, M. Geddo, G. Iadonisi, D. Ninno, Phys. Rev. B **43**, 5296 (1991).
18. G. Iadonisi, F. Bassani, Il Nuovo Cimento **2**, 1541 (1983); G. Iadonisi, V. Marigliano, Il Nuovo Cimento **6**, 193 (1985); G. Strinati, J. Math. Phys. **28**, 981 (1987); G. Iadonisi, F. Bassani, G. Strinati, Phys. Stat. Sol. **153**, 611 (1989); G. Iadonisi, M. Chiofalo, V. Cataudella, D. Ninno, Phys. Rev. B **48**, 12966 (1993).
19. W. van Haeringen Phys. Rev. **137**, 1902 (1965).
20. A.B. Migdal, Sov. Phys. JETP **34**, 996 (1957).
21. G.M. Eliashberg, Sov. Phys. JETP **11**, 696 (1960).
22. J.K. Lindhard, Dan. Vidensk. Selsk. Mat. Fys. Medd. **28**, 8 (1954).
23. J. Hubbard, Proc. R. Soc. London A **243**, 336 (1957).
24. A.L. Fetter, J.D. Walecka, *Quantum theory of many-particle systems* (McGraw-Hill Book Company, 1971).
25. L. Hedin, Phys. Rev. **139**, A796 (1965).
26. B.I. Lundqvist, Phys. Status Solidi **32**, 273 (1969).
27. J.J. Quinn, R.A. Ferrel, Phys. Rev. **112**, 812 (1958).
28. E. Kartheuser, in *Polarons in Ionic Crystals and Polar Semiconductors* (North-Holland, Amsterdam, 1972), p. 717.
29. W.B. da Costa, N. Studart, Phys. Rev. B **47**, 6536 (1993).
30. S. Engelsberg, J.R. Schrieffer, Phys. Rev. **131**, 993 (1963).
31. S. Das Sarma, A. Kobayashi, W.Y. Lai, Phys. Rev. B **36**, 8151 (1987).
32. D. Pines, *Elementary excitations in Solids* (Benjamin, 1963).
33. N.D. Mermin, Ann. Phys. **18**, 421, 454 (1962).
34. L.P. Kadanoff, P.C. Martin, Phys. Rev. **124**, 670 (1961).
35. T. Kostyrko, R. Micnas, Phys. Rev B **46**, 11025 (1992); T. Kostyrko, Phys. Stat. Sol. b **143**, 149 (1987).
36. We have checked that the calculated spectral weight function satisfies the sum rule: $\int_{-\infty}^{+\infty} d\omega A(k,\omega) = 1$ very well.
37. G. Iadonisi, M. Chiofalo, V. Cataudella, D. Ninno, Phys. Rev B **48**, 12966 (1993); G. Capone, V. Cataudella, G. Iadonisi, D. Ninno, Il Nuovo Cimento D **17**, 143 (1995).
38. J.M. Luttinger, Phys. Rev. **119**, 1153 (1960).
39. T.M. Rice, Ann. Phys. **31**, 100 (1965).